# I/O SYSTEM DESIGN FOR THE PSYONIC ADVANCED BIONIC HAND

By

Byron Hopps

Steven Sun

Final Report for ECE 445, Senior Design, Fall 2017

TA: Zipeng “Bird” Wang

12 December 2017

Project No. 28

# Abstract

This report details the design of a system to add convenient user interfaces to the PSYONIC Advanced Bionic Hand. The Input/Output System, or I/O System, adds a USB Type-C port for battery charging and wired data transmission. An onboard Bluetooth radio lets the I/O System take commands from an app on the user's smartphone, providing an easy and convenient way for patients and clinicians to access and configure the software of the prosthetic hand. The USB Power Delivery protocol is used so the input voltage can be raised to up to 20 V, increasing input power and decreasing battery charge times. Lastly, an onboard Battery Management System charges a lithium-ion battery, ensures that it is always being operated within its safe operating area, and disconnects the battery in case of an error.

# Contents

# 1 Introduction

There are 11.4 million hand amputees in the world, and over 80% are in developing nations [1]. Less than 3% of these amputees have access to the rehabilitation necessary to rebuild the functionality they lost by losing a limb [2]. The prohibitive cost of existing prosthetics makes them unaffordable to amputees in developing nations. Most low-cost designs for prosthetic hands focus on the mechanical design of the hand, not on the design of an integrated system that is a viable product for amputees [3].

PSYONIC is a startup at the University of Illinois that is working to fix these issues by developing a low-cost prosthetic hand for use on amputees worldwide, in both developed and developing nations. They are working alongside clinicians and amputees to ensure that the hand will meet the needs of amputees. With features such as control by electromyographic (EMG) pattern recognition and tactile feedback through use of electrotactile stimulation, the PSYONIC Advanced Bionic Hand will be a serious competitor to existing prosthetic hands on the market today [4]. Their prototypes have reached a high level of functionality, and they are now moving the design towards production hardware [5]. While the core functionality of the hand is well-integrated, auxiliary functionality such as battery charging and external I/O are either nonexistent or require specialized hardware to be used.

We plan to design a new system for PSYONIC's prosthetic hand, to be known as the I/O system. This system will integrate all the external I/O necessary for the prosthetic arm. It will contain two external interfaces, namely USB type-C and Bluetooth. USB type-C allows for rapid battery charging and wired data communications. Bluetooth enables the hand to be capable of low-speed wireless data transfer, providing a convenient interface for patients. The USB data interface lets the hand rapidly transfer uncompressed data for use by clinicians or researchers. These interfaces will let us build an API that will let us, and more importantly, clinicians perform a variety of remote control and configuration tasks. This includes the ability to query and write values that control various aspects of the hand's operation, such as the finger speed sensitivity or the battery charge level. While there are commercial solutions for individual aspects of this problem, there is no commercially available solution that can perform all the required functionality.

## 2 Design

The I/O System supplies power to the prosthetic hand, communicates with external devices through a wired USB connection or a wireless Bluetooth connection, and sends commands to the rest of the hand. It consists of two physical modules, the I/O Board and a 2.2Ah lithium-ion battery, as shown in Figure 1. The power supply powers the prosthetic hand, taking power from a USB type-C connector and storing it in a battery. Through use of the USB Power Delivery (USB-PD) protocol, a higher input power can be achieved. A lithium-ion Battery Management System (BMS) controls the power flow to and from the battery. The communications interfaces exchange data with external Bluetooth and USB devices, sending commands and data to the hand to the PSYONIC Advanced Bionic Hand through a Universal Asynchronous Receiver Transmitter (UART), also known as a serial port. The USB Serial Interface converts the USB protocol to a serial connection, and the Bluetooth Module contains both a Bluetooth transceiver and the main microcontroller for the I/O Board. The Serial Multiplexer, or UART Mux, selects whether the USB interface or the Bluetooth interface is controlling the hand. Lastly, the radiofrequency (RF) front end contains an antenna and matching network required for the I/O Board to communicate wireless over Bluetooth.

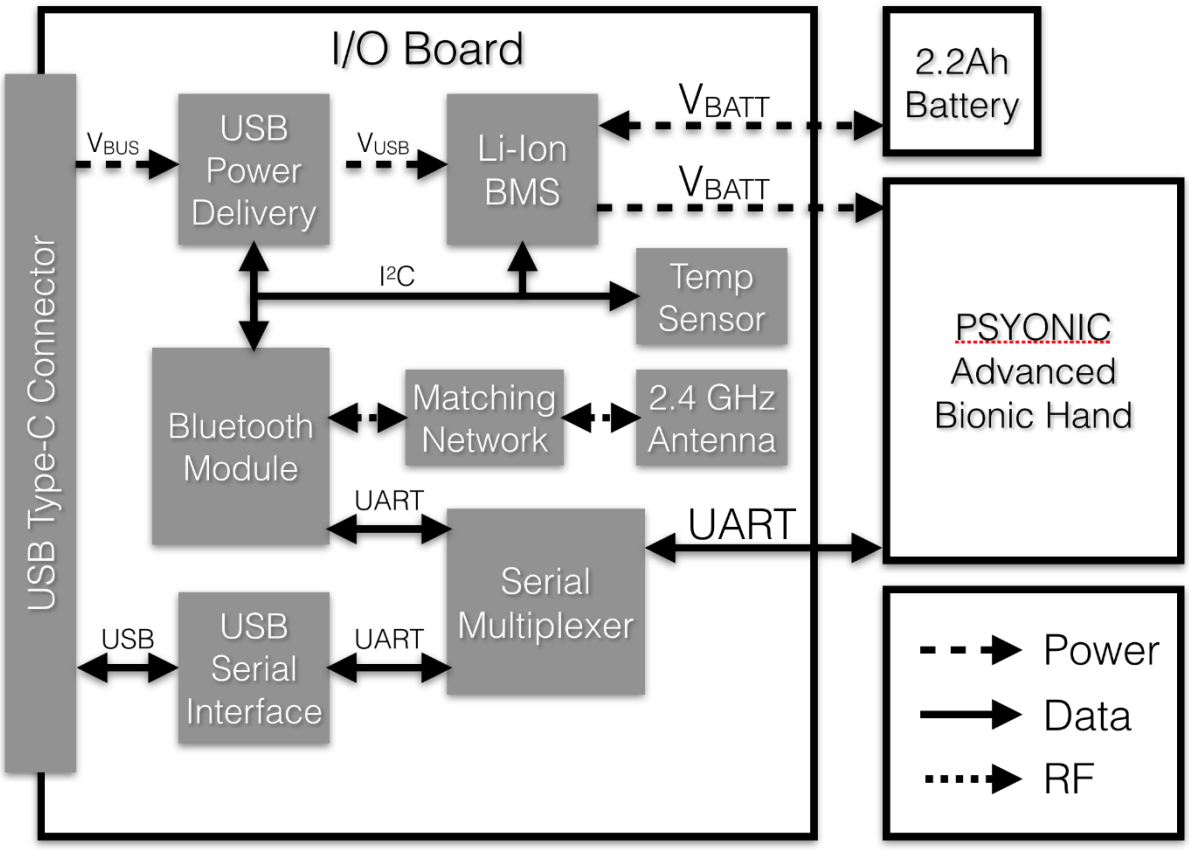


Figure 1: System Block Diagram

## 2.1 USB Type-C Connector

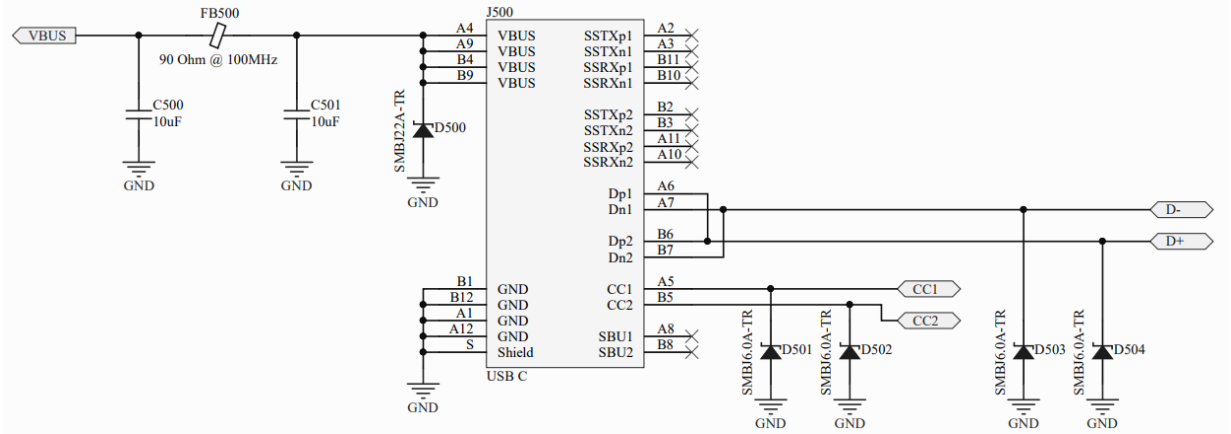


Figure 2: USB Type-C Connector Schematic

The USB Type-C connector shown in Figure 2 is the main external interface for the I/O Board. Transient Voltage Suppression (TVS) diodes were selected with the intention of preventing an ESD event from damaging circuitry downstream from the USB port; however, the diodes selected for the data lines and Configuration Channel (CC) had too much capacitance for proper functionality. Depopulating the diodes on the I/O Board fixed this problem. Additionally, a ferrite bead Pi filter is present on the USB VBUS line to suppress conducted emissions from propagating along VBUS. The pin configuration used here follows the recommendations in the USB Type-C specification for a USB 2.0 device with power delivery [6] [7].

## 2.2 Serial Multiplexer

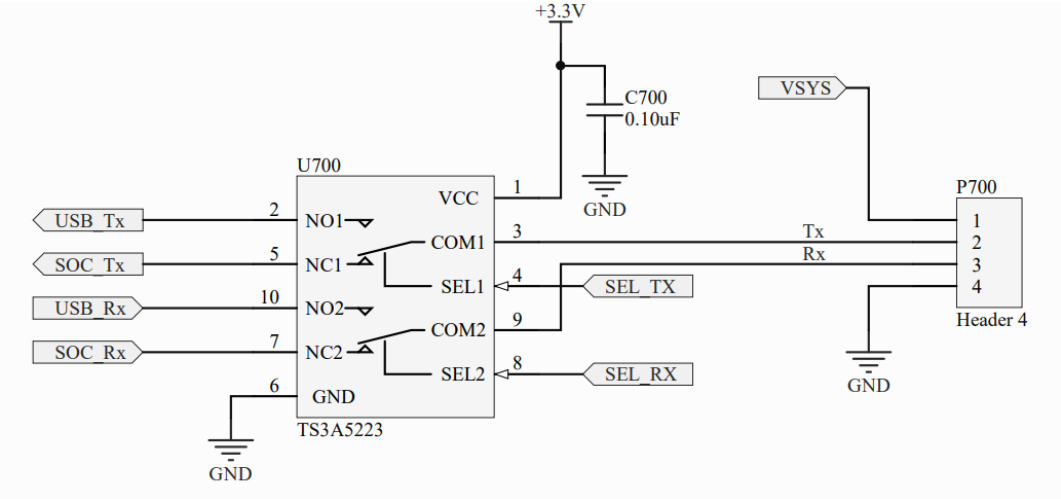


Figure 3: Serial Multiplexer Schematic

An analog switch was used to select whether the hand should accept commands from the Bluetooth Module or the USB data interface, as shown in Figure 3. This change greatly simplifies software development, allowing the Bluetooth Module to focus on tasks other than passing data from one interface to another.

## 2.3 USB Power Delivery Negotiator

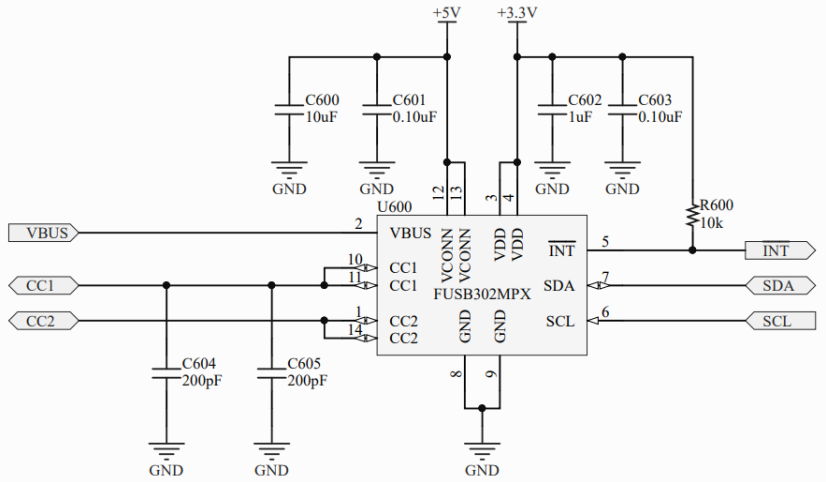


Figure 4: USB-PD Negotiator Schematic

The implementation of the USB-PD negotiator in Figure 4 follows the recommended application schematic in the FUSB302 datasheet [8]. Data is sent between the Bluetooth Module and the USB-PD Negotiator over an $I^2C$ bus, with an extra interrupt line to inform the Bluetooth Module is a new packet has arrived. Input overvoltage and transient protection circuity for the USB Configuration Channel is described in Section 2.1.

## 2.4 Lithium-Ion Battery Management System

The circuitry for the Lithium-Ion Battery Management System (BMS) shown in Figure 5 generally follows the application diagram from the BQ25703 datasheet [9]. The BQ25703 variant of the BQ25700 was chosen due to the former having a plain $I^2C$ bus instead of the more advanced SMBus. The lower half of Figure 5 consists of passive components whose values are specified in the datasheet [9]; however, the upper half contains the power path of the BMS, where we took care in selecting components that would ensure high system performance.

The BMS consists of a Buck-Boost switchmode voltage regulator with an additional series P-Type Metal Oxide Field Effect Transistor (MOSFET) on the converter output to gain control over the battery current. The CSD17579Q5AT N-Type MOSFETs were selected as the main switches for the Buck-Boost Converter due to their low on-state resistance and gate charge, the combination of which increases converter efficiency.

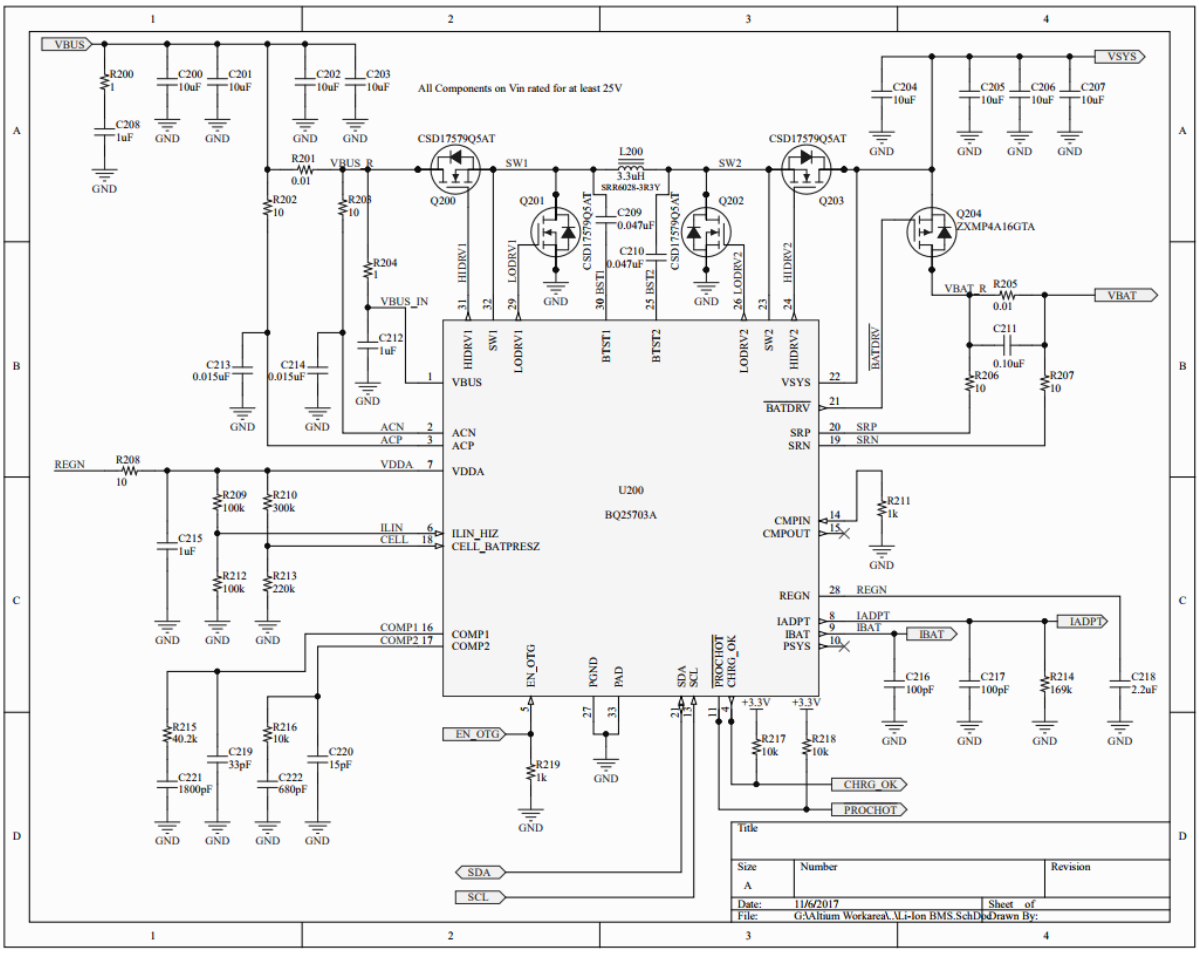


Figure 5: Lithium-Ion Battery Management System Schematic

## 2.5 USB Serial Interface

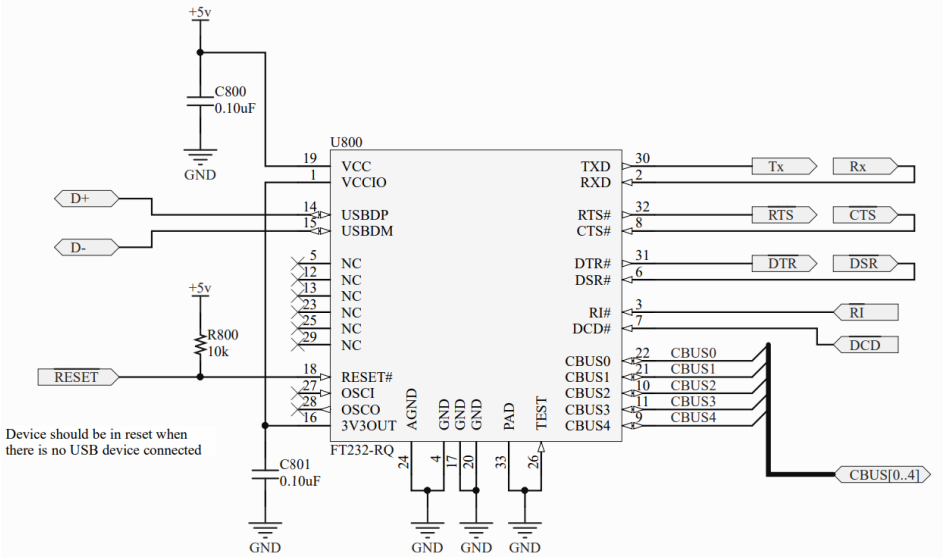


Figure 6: USB Serial Interface Schematic

The FT232-RQ was selected as the USB-to-Serial converter due to its ubiquity in this application. Figure 6 contains the implementation of the FT232-RQ, with all RS-232 handshaking and control signals broken out to allow the use of hardware handshaking.

## 2.6 Bluetooth Module and Matching Network

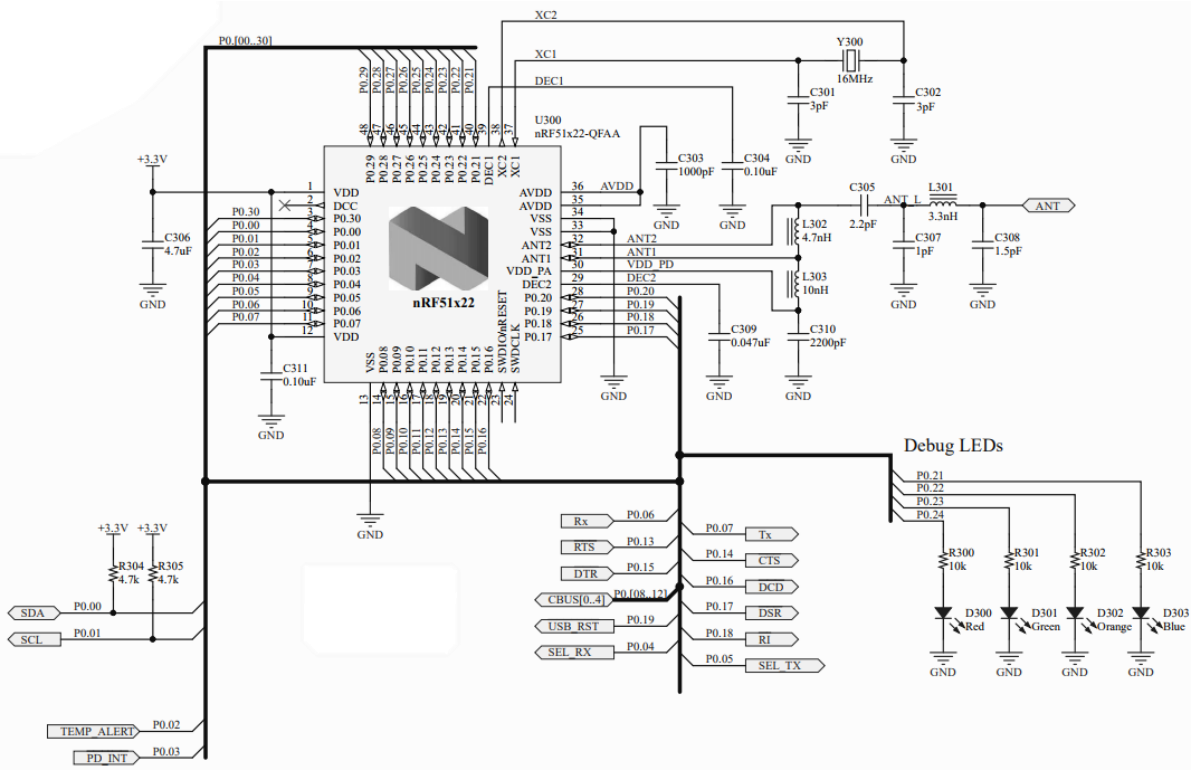


Figure 7: Bluetooth Module Schematic

The Bluetooth Module is shown in Figure 7. It controls the other peripherals on the I/O Board and communicates with the hand unless the USB port is active. The NRF51822 was selected as the Bluetooth Module due to excellent support resources and a variety of relevant on-chip peripherals. We added a 16 MHz crystal oscillator since it is required to operate the Bluetooth radio [10], and decided to not implement the low frequency 16.786 kHz crystal oscillator to save board area. To ease firmware development, four colored Light Emitting Diodes (LEDs) were added.

Figure 7 also contains the antenna matching network, which uses a lumped-element implementation. Components for the matching network were selected so that their self-resonant frequency was at least twice as high as the frequencies of interest (2.4 GHz), to reduce the potential for non-ideal components to cause the design to work other than as intended.

## 2.7 2.4 GHz Antenna

Due to the challenges of successfully designing a PCB trace antenna, an external antenna was used to reduce the change of a design error causing the I/O Board to not work properly. An Ultra-Miniature

Coaxial (UMC) connector was selected for the antenna connector to reduce the board footprint of the antenna connector.

## 2.8 Temperature Sensor

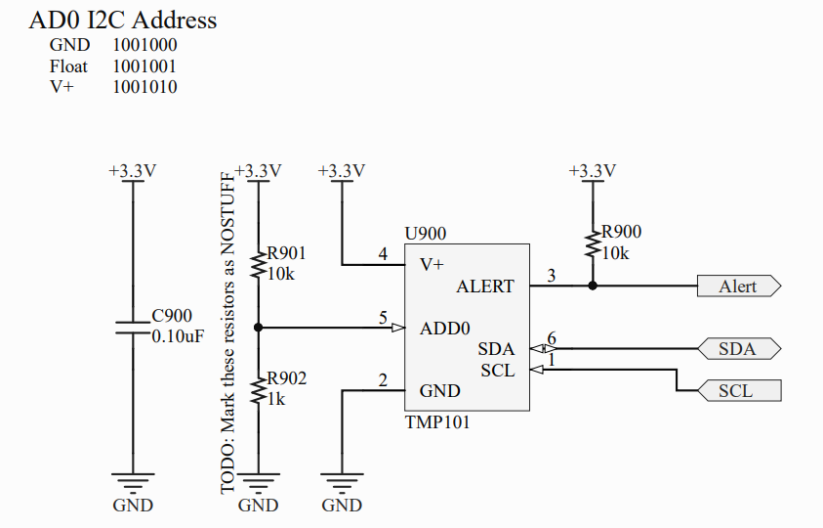


Figure 8: Temperature Sensor Schematic

The circuit shown in Figure 8 is the implementation of the TMP101, an $I^2C$ temperature sensor. A temperature sensor was added due to the possibility of the hand being used in conditions outside the safe operating range of the hand's lithium-ion battery. Adding a temperature sensor allows the I/O Board to determine if the battery is too cold or too hot and disable it if needed. An alert signal can generate an interrupt if the temperature goes outside of a programmable range [11].

## 2.9 Voltage Regulators

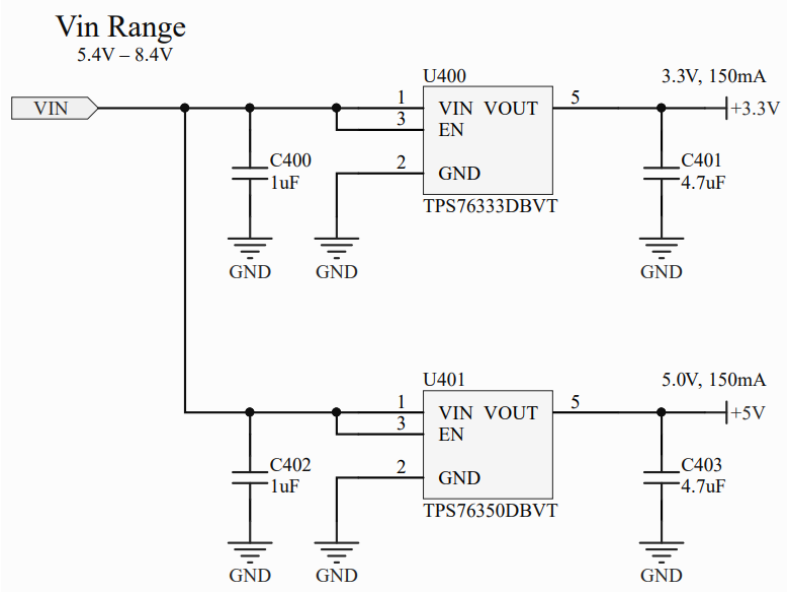


Figure 9: Voltage Regulators Schematic

The TPS763xx series of Low-Dropout linear regulators (LDOs) were selected to perform onboard voltage regulation. There are two fixed-output regulators, a 3.3 V and a 5.0 V regulator; each can supply 150 mA [12]. They provide the voltage rails necessary to power the rest of the circuitry on the I/O Board.

# 3 Design Verification

## 3.1 Bluetooth Data Interface

To verify that the Bluetooth Data Interface, we used the iPhone App we developed. The serial output from the I/O Board was attached to a logic analyzer to capture the messages being sent. Figure 10 contains the data recorded. We were able to successfully send and receive data between the prosthetic hand and a smartphone, meeting the requirements we set.


Figure 10: Bluetooth Data Transfer

The test was repeated successfully with the iPhone 30 feet away from the I/O Board, to verify that the RF front end had a low enough insertion loss that it supported a reasonable communication range. Unfortunately, we were not able to verify the requirements for the RF front end directly, as the senior design lab lacked the equipment to do so. The equipment we needed was an RF differential probe with a 3 dB bandwidth of at least 5 GHz and a SMA to Type-N RF connector adapter.

## 3.2 USB Data Interface

We tested the USB Data Interface with two computers. One was attached to the I/O Board's USB Type-C port, and the other used a USB-to-Serial converter to connect to the hand serial port on the I/O Board. Next, we opened a serial terminal on both computers with the baud rate set to 115200. We then verified that we were able to send data between the two computers by typing words on each terminal, and verifying that the words were displayed on the other computer. Durin1g this test, the I/O Board was powered from the USB Type-C port.

## 3.3 USB Power Delivery

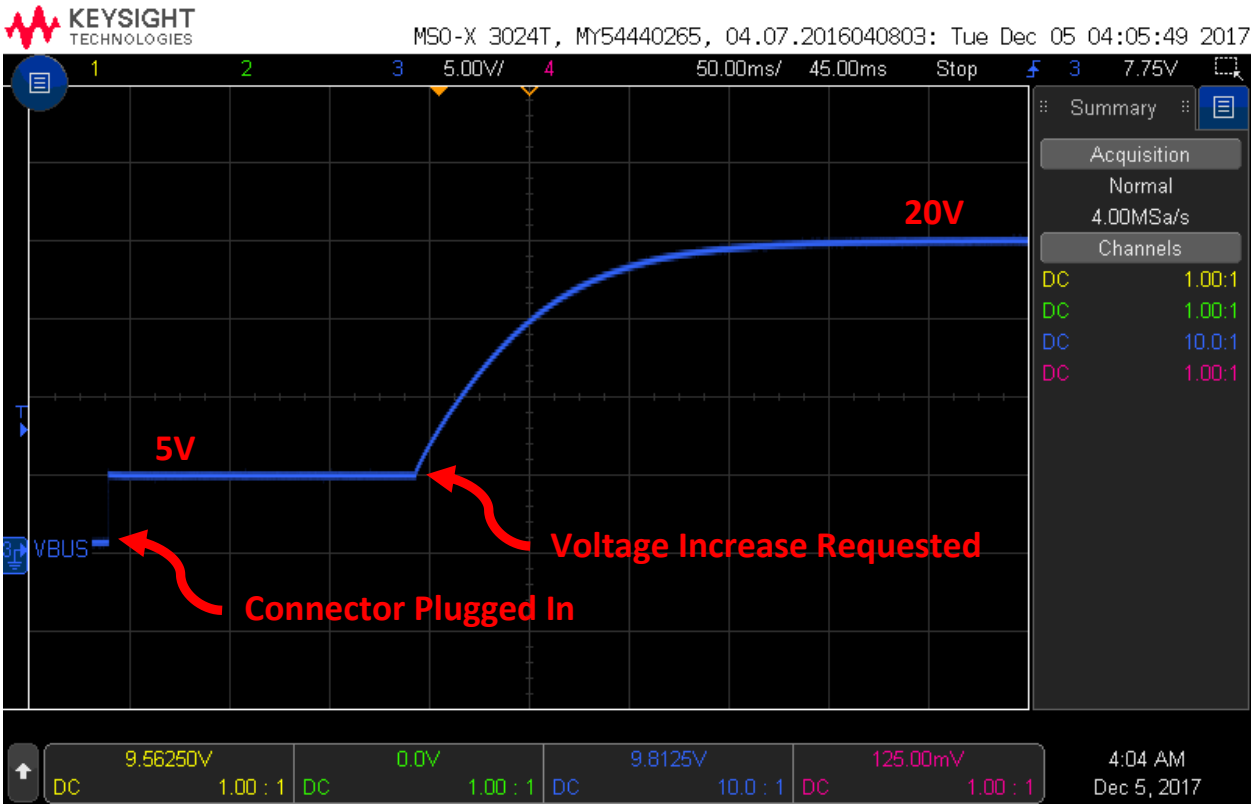


Figure 11: USB Power Delivery Voltage Increase

To test that the USB Power Delivery Negotiator could increase the supply voltage, we attached the I/O Board to a Samsung brand USB Power Delivery enabled wall charger. We were able to successfully communicate with the wall charger and request a larger bus voltage, as demonstrated in Figure 11.

## 3.4 Battery Management System

To verify the functionality of the BMS, a series of tests were conducted to verify each requirement.

### 3.4.1 Input Voltage Range

To verify the BMS input voltage range, we attached a programmable load set to constant voltage mode to the BMS. This caused the BMS to sink a 1 A charging current into the programmable load for the duration of the test. We then used a power supply as the input voltage, raising it from 5 V to 20 V in 1 V increments. At each point we recorded the battery output voltage, which is displayed in Figure 12.

Over the entire input voltage range, the output voltage varies by less than 100 mV. At all times the BMS was sinking 1 A into the programmable load, verifying that the BMS can charge a battery across the entire voltage range.

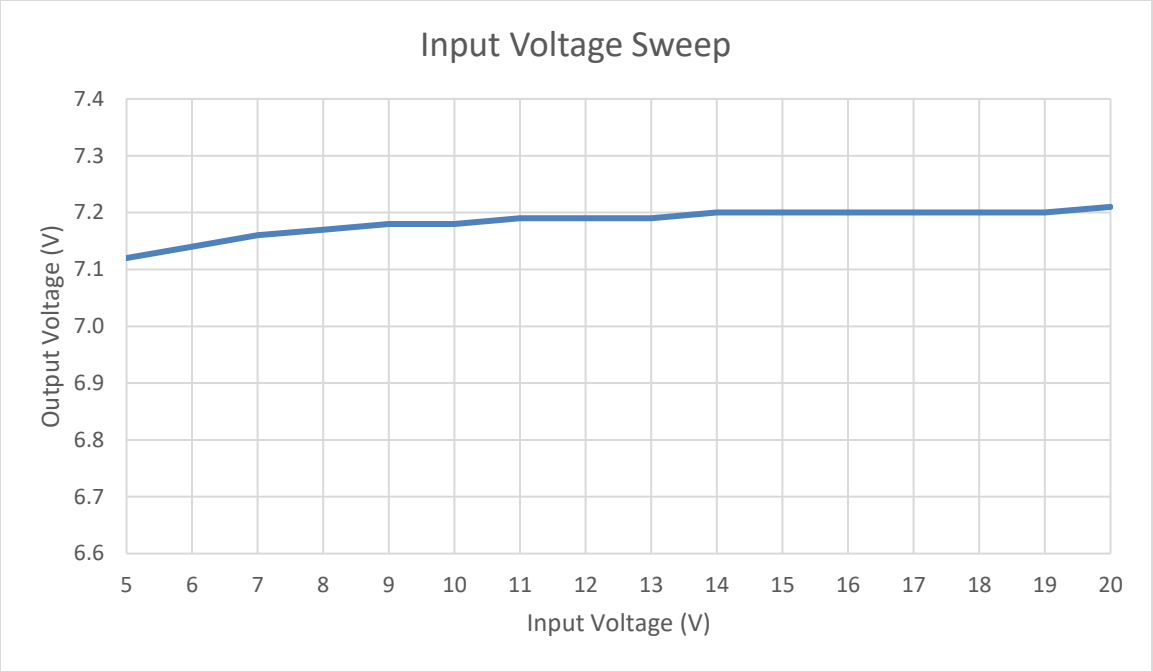


**Figure 12: BMS Input Voltage Sweep**

### 3.4.2 Battery Charge Current

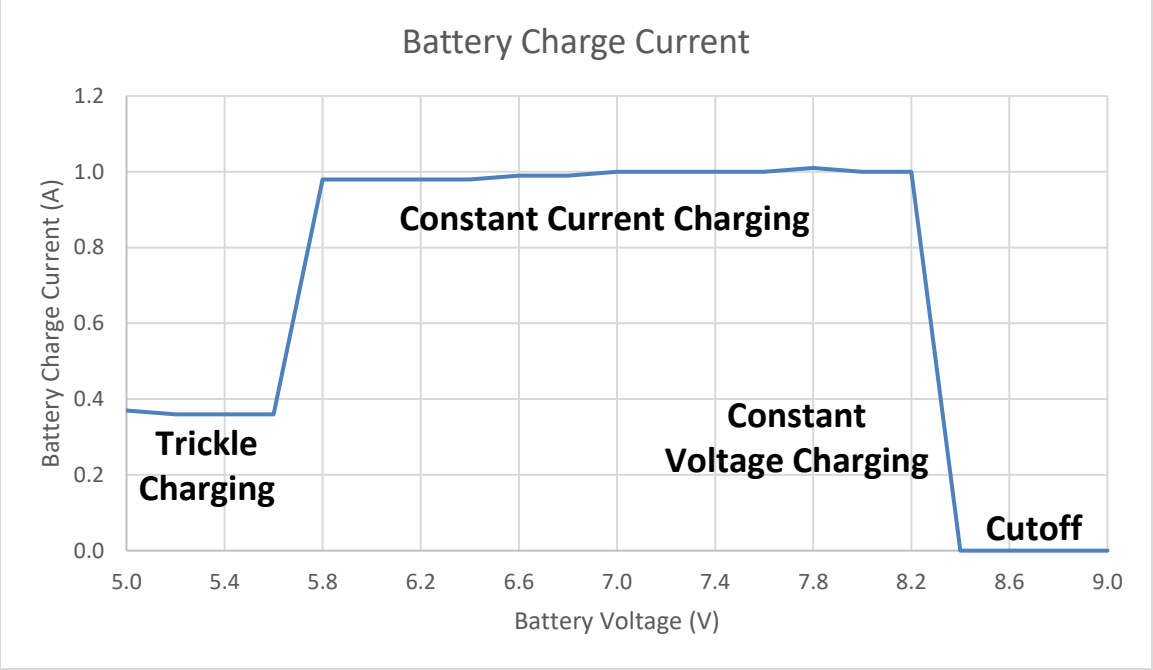


**Figure 13: BMS Battery Charge Current**

To verify that the BMS can charge the battery safely, we attached the BMS to a programmable load set to constant voltage mode. Using a programmable load allowed us to avoid having to test with an actual battery until we were certain that our charging circuitry was safe. With a 20 V input voltage from a

power supply, we swept the battery voltage from 5.0 V to 9.0 V in 0.2 V increments. The results of our sweep can be found in Figure 13.

As shown in Figure 13, there are four modes of operation. Trickle charging occurs when the battery voltage is very low. The BMS applies a small charge current (around 370 mA) to see if the battery can be charged. If the battery can be charged, the BMS proceeds to the constant current charge mode. Otherwise, the BMS stops charging the battery. In the constant current charge mode, the BMS applies a 1 A current to the battery. As the battery voltage reaches 8.4 V, the charging current is tapered off while holding the battery voltage steady at 8.4 V. This is the constant voltage charging mode. Lastly, if the battery voltage is too high, the BMS enters the cutoff mode, where the battery is fully disconnected from the rest of the system.

### 3.4.3 Output Short Circuit

The BMS is configured with a current limit, and will shut off if the current limit is exceeded. To verify this, we attached a 7 V source to the battery terminals to avoid having to use an actual battery for this test. We then attached a programmable load to the system voltage output, set to sink a constant current of 750 mA. We then changed the programmable load settings to attempt to maintain a constant voltage of 50 mV, simulating a load short. When we did so, the BMS disconnected the battery from the load, resulting in a battery current of 0 A.

## 3.5 Lithium-Ion Battery

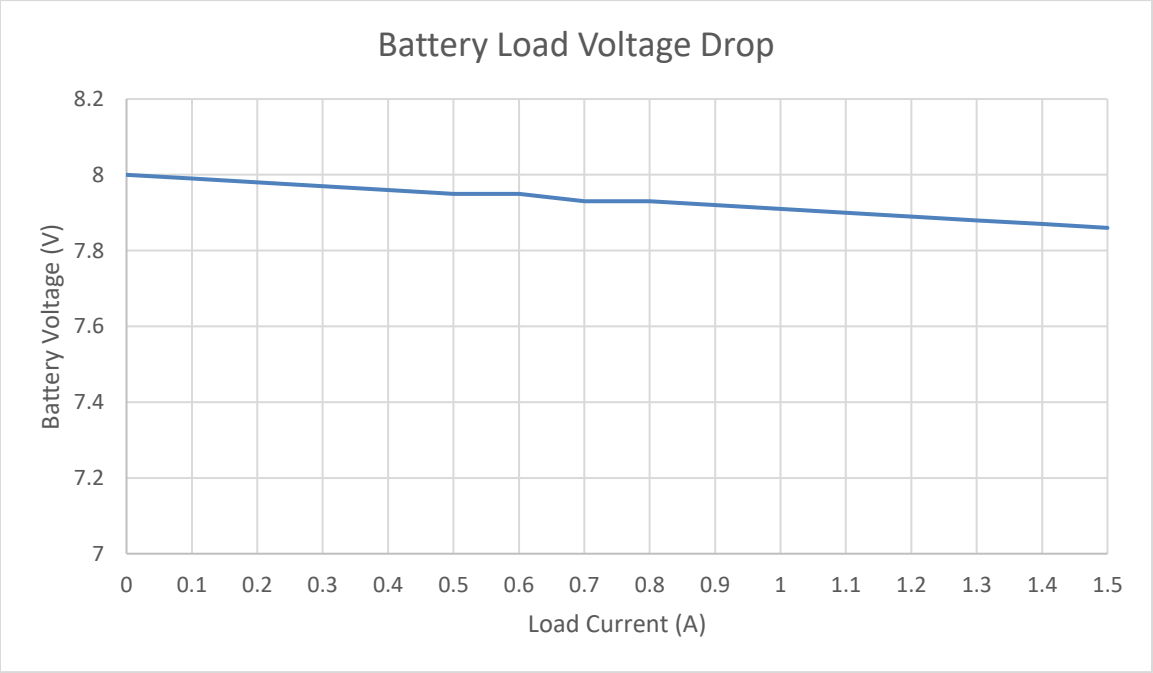


**Figure 14: Battery Load Voltage Drop**

To measure the discharge characteristics of the Lithium-Ion battery, we attached the battery to a programmable load. The battery had an open circuit voltage of 8 V. We then increased the battery load current from 0 A to 1.5 A in 100 mA intervals, measuring the battery voltage at each point. The results

are plotted in Figure 14. At a load current of 1 A, the battery voltage was 7.91 V, which is a 90 mV decrease from the open circuit voltage, meeting the battery discharge requirement.

# 4 Costs

The total cost to develop this project and assemble 1000 units is $55,730.

## 4.1 Parts

Table 1 contains the part cost breakdown for the I/O Board. Due to the large quantity of individual circuit components, only the total costs are presented in this section. The entire Bill of Materials (BOM) for the I/O Board can be found in Appendix B. We spent no money on PCBs, since we participated in the course PCB purchases. Similarly, we spent no money on the lithium-ion batteries, as we used the ones that PSYONIC already had on hand. In total, a total of $173.90 was spent on this project.

**Table 1: Part Costs**

| Description | Manufacturer | Cost (Qty. 5) | Cost (Qty. 1k) | Amount Spent |
|---|---|---|---|---|
| Circuit Components | Multiple (See Appendix B) | $33.48 | $15.42 | $166.40 |
| PCB Assembly | PCBway | $10.00 | $0.51 | $0.00 |
| Lithium-Ion Battery | Hobby King | $4.28 | $4.28 | $0.00 |
| Bluetooth Antenna | Adafruit Electronics | $2.50 | $2.00 | $7.50 |
| **Totals** | | **$45.98** | **$17.93** | **$173.90** |

## 4.2 Labor

Our labor costs are estimated with an hourly rate of $45/hour. We both worked an average of 12 hours each week, and the project lasted for 14 weeks of serious development. This results in an estimated development cost of $37,800.

$$2\ people * \frac{\$45}{hr} * \frac{12\ hr}{wk} * 14\ wk * 2.5 = \$37{,}800$$

# 5 Conclusion

Overall, we were successful in accomplishing the goals of our project. We were able to demonstrate all core functionality of the I/O Board, and create something that will be of use to PSYONIC in the future.

## 5.1 Accomplishments

Our project involved many different interconnected circuit blocks, each with their own set of difficulties. The schematic for the I/O Board was ten pages long, and many of those pages were non-trivial to design and implement. The I/O Board contains switchmode power electronics, RF circuity, and high-speed serial links. The BMS contains a switchmode Buck-Boost converter with a switching frequency of 800 kHz, and is capable of handling 10 W with minimal losses. The maximum power is closer to 60 W, although we did not heavily test the circuit with that configuration. There is a fully featured Bluetooth radio, which requires an RF matching network capable of 2.4 GHz operation with a range greater than 30 feet. Lastly, the USB interface is a 12 MHz high-speed digital link, which also requires some extra design attention to ensure proper signal integrity. All circuitry on the I/O board was designed by us; no premade modules were used in this project.

The PCB itself is also worthy of mention. With dimensions of 4 cm by 5 cm, it is one of the smallest boards designed this semester. It also has one of the highest BOM counts, with 117 components on the I/O Board. Very small components were used to achieve such a high component density, making it more difficult to solder. All boards were hand soldered with a soldering iron and a hot air rework tool. The PCB layout still managed to stay within the widest tolerances available for trace width, spacing, and other parameters, even though we had a high component density. Also noteworthy is that we only had to design one revision of the I/O Board; all the circuitry worked properly without needing major modifications.

We went above and beyond the project requirements when writing the software. We wrote an iPhone App to demonstrate the Bluetooth interface, which was not part of the project requirements. Since neither of us knew how to develop an App before this semester, we had to learn how to do so as part of the project. Firmware was developed to implement the USB Power Delivery and Bluetooth Low Energy protocols. Additionally, we developed low level driver to interface with the many programmable integrated circuits on the I/O Board.

Lastly, we managed to complete this project despite some major scheduling difficulties. Steven is a sophomore who was concurrently enrolled in ECE 391 this past semester, which is the most time-consuming course offered by the ECE department. He also was involved with other PSYONIC projects. Byron was abroad in Australia for over four weeks racing a solar-powered across the Australian Outback. While abroad, he helped write the Project Proposal, Design Document, and drove over 100 km around 3:00 AM one night to find cell service so he could phone into the Design Review. Unfortunately, he was not able to get much work done on the I/O Board schematics while abroad, so he designed the entire board once he got back. (The projected was divided so that Byron did the hardware design and Steven wrote the software.) Despite these scheduling difficulties, we were able to successfully create and program an impressive piece of electronics.

## 5.2 Uncertainties

There are always some things that don't work properly on the first board revision, and this project was no different. We had a few different things that didn't work properly when we assembled the I/O Board for the first time. When writing the software for the USB Power Delivery and the Bluetooth radio, we discovered that the Bluetooth Module didn't have enough computer power to run both the USB Power Delivery and Bluetooth Low Energy at the same time. However, we were able to write software to make them work on their own. This means that when the Bluetooth interface doesn't work when a USB cable is plugged in, and vice versa.

The second issue we had was that there were no pullup resistors on the serial lines going to and from the rest of the prosthetic hand. This resulted in the receiver generating random data when no device was plugged into the serial port, making it difficult to determine whether a device is attached to the port or not.

We also had some issues with electro-static discharge (ESD) protection diodes. The ESD diodes that we selected for the USB data lines and USB Configuration Channel lines had too much capacitance, resulting in the USB interface not working. To fix the problem, we desoldered the ESD diodes, which fixed the issue, although it left the USB interface vulnerable to an ESD event. Another potential issue is that we didn't put ESD diodes on the serial port to the prosthetic hand. While this didn't cause any problems, it does create the potential for problems to arise later.

Lastly, there is one instance where a logic signal pulled up to 5 V is connected directly to the Bluetooth Module, which is a device that operates on 3.3 V logic. This creates the potential for the 5 V signal to damage the Bluetooth Module by overvoltage. While we were able to get the Bluetooth Module to work properly, we did run into problems where the Bluetooth Module would stop working every now and then, and this is likely the reason why they stopped working randomly. Since the signal is driven by the Bluetooth Module, this problem can be fixed by adding a N-Type MOSFET to pull down the 5 V signal.

It's worth mentioning that while we did have a few hardware problems, none of them prevented us from meeting the requirements and successfully demonstrating our project, and that none of them required us to cut traces or create new traces with fine wire.

## 5.3 Ethical Considerations

The main safety hazard with our project is the lithium-ion battery used to power the hand. If not properly managed, it has the potential to outgas and catch fire. The only way to put out a lithium-ion battery fire is to wait until it burns out. Battery fires can be avoided by keeping the battery within the safe operating area, as defined by the manufacturer. This generally entails keeping the battery voltage above 2.7V and below 4.2V, as well as keeping the cell temperature between 0ºC and 45ºC during charging. Wider temperature ranges apply during discharge and storage. This is known as the safe operating area of the lithium-ion cell [13]. A series of requirements have been written to verify that our BMS keeps the battery within its safe operating area, and the verification procedures do not use an actual battery to prevent a battery fire in case the BMS does not meet our requirements. This is in

accordance with the first and ninth item on the IEEE code of ethics [14], as an improperly designed battery management system has the potential to cause serious harm.

Another aspect of our project is that it is intended for use in a medical device. This gives our project a greater potential to do harm to people. As a medical device, our project will be regulated by the Food and Drug Administration (FDA), which means that our project will need to meet strict testing requirements. We will be documenting all the tests we do on the I/O System to support the FDA approval process to help PSYONIC gain FDA approval for the PSYONIC Advanced Bionic Hand. All tests will be carried out and accurately documented, as falsifying test data is a serious ethical violation [14].

Our project adds the capability to configure the prosthetic hand remotely. This raises the possibility of an unauthorized individual gaining access and doing things against the wishes of the user. The Bluetooth Protocol's built in encryption and associated device pairing access model process mitigates these concerns. Even then, we only implemented features that will not result in sudden and unexpected changes to the hand's behavior.

Lastly, our project includes an intentional emitter of electromagnetic radiation in the form of a Bluetooth radio module. It will also contain moderately high-speed digital busses and multiple switch-mode circuits. These circuits have the potential to cause unintentional RF emissions. The electromagnetic spectrum is a shared resource by all of humanity, and the noise floor has been steadily increasing due to the proliferation of circuitry which have not been designed with electromagnetic interference (EMI) concerns in mind. In the USA, the Federal Communications Commission (FCC) requires that all products sold in the USA pass unintentional emissions testing. We will keep EMI considerations throughout the design process, especially during PCB layout, to ensure that our design meets FCC regulations.

## 5.4 Future work

Moving forward, our goal is to mechanically integrate the I/O Board into the hand itself. This will likely require that the board's shape be modified to fit into a smaller area, and that connectors get moved around to facilitate easy access without opening the hand. The next revision of the I/O Board will also incorporate small tweaks and revisions to increase the resilience and reliability of the hardware as well as simplifying software development.

We are also considering changing the Bluetooth chipset used to use Bluetooth version 5 (BT5) instead of Bluetooth Low Energy (BLE). BT5 gives us four times the data rate using half as much power as BLE. However, BT5 is a very new standard; we would like to wait and make sure that many devices on the market support it before we make the switch.

On the software side, the iPhone App we developed has a functional user interface that could use a lot of cleaning up and reworking to make it aesthetically pleasing. We would like to take some time to make the App something that is of sufficient quality and usability that it could be released to patients and clinicians worldwide. The firmware for the I/O Board could also use some cleanup and consolidation to improve future maintainability and reliability.

Beyond that, it is important that we start to research the FDA approval process. We need to know what tests and documentation will be needed to gain approval, and determine if any architecture changes will be necessary to ease approval. Rewriting parts of the firmware to meet a coding standard will likely be necessary as well.

# References


[1] World Health Organization, "World Report on Disability," World Health Organization, New York, 2011.

[2] D. Cummings, "Prosthetics in the developing world: a review of the literature," *Prosthetics and Orthotics International,* no. 20, pp. 51-60, 1996.

[3] P. Slade, A. Akhtar, M. Nguyen and T. Bretl, "Tact: Design and performance of an open-source, affordable, myoelectric prosthetic hand," *IEEE International Conference on Robotic Automation (ICRA),* pp. 6451-6456, May 2015.

[4] A. Akhtar, K. Y. Choi, M. Fatina, J. Cornman, E. Wu, J. Sombeck, C. Yim, P. Slade, J. Lee, J. Moore, D. Gonzales, A. Wu, G. Anderson, D. Rotter, C. Shin and T. Bretl, "A low-cost, open-source, compliant hand for enabling sensorimotor control for people with transradial amputations," in *IEEE 38th Annual International Conference of the Engineering in Medicine and Biology Society*, Orlando, 2016.

[5] PSYONIC, "Technology," [Online]. Available: http://www.psyonic.co/technology/. [Accessed 19 September 2017].

[6] USB Implementers Forum, *Universal Serial Bus Type-C Cable and Connector Specification,* 2016.

[7] USB Implementers Forum, *Universial Serial Bus Power Delivery Specification,* 2016.

[8] ON Semiconductor, "FUSB302 Programmable USB Type-C Controller with Power Delivery," 2015.

[9] Texas Instruments, *Multi-Chemistry Battery Buck-Boost Charge Controller With System Power Monitor andProcessor Hot Monitor,* 2017.

[10] Nordic Semiconductor, *nRF51822 Product Specification,* 2014.

[11] Texas Instruments, "TMP10x Temperature Sensor With I2C Interface with Alert Function," 2002.

[12] Texas Instruments, "TPS763 Low-Power 150-mA Low-Dropout Linear Regulators," 1998.

[13] D. Andrea, Battery Management Systems for Large Lithium Ion Battery Packs, Norwood, MA: Artech House, pp. 6-7.

[14] IEEE, "IEEE Code of Ethics," June 2017. [Online]. Available: https://www.ieee.org/about/corporate/governance/p7-8.html. [Accessed 20 September 2017].

# Appendix A. Requirements and Verification Table

**Table 2: Requirements and Verification**

| Requirement | Verification | Status |
|---|---|---|
| The USB-PD Controller shall select the output voltage with the maximum available power or voltage to provide highest efficiency and remain compatible with variety of chargers on the market | 1. Attach a power adapter to the I/O Board<br>2. Verify that the output voltage is 5V<br>3. Instruct the USB-PD negotiator to select the optimal output configuration<br>4. Apply the maximum load to the power output<br>5. Verify that the VBUS voltage is what was reported by the adapter<br>6. Repeat this procedure with power adapters from well-known companies such as Apple, Samsung, and Google | Verified (Section 3.3) |
| The Lithium-Ion battery shall be able to sustain a continuous discharge current of 1 amp with a voltage drop of at most 100mV | 1. Measure the battery voltage<br>2. Attach the battery to a programmable load<br>3. Set the load current at 1A<br>4. Measure the battery voltage under load<br>5. Verify that the difference between the two measured voltages is less than or equal to 100mV | Verified (Section 3.5) |
| The BMS shall change the battery from an input voltage range of 5V to 20V, inclusive | 1. Attach a power supply to the BMS input<br>2. Attach a programmable load set to maintain a constant voltage in place of the battery<br>3. Sweep the input voltage from 5V to 20V<br>4. For each input voltage, verify that the BMS battery output voltage is correct | Verified (Section 3.4.1) |
| The BMS shall charge the battery with a maximum charge current of at least 750mA, with a preferred value of 1.1A | 1. Attach a power supply to the BMS input<br>2. Attach a load in place of the battery<br>3. Measure the load current | Verified (Section 3.4.2) |
| The BMS shall not charge the battery when the pack voltage is greater than 8.4V or less than 5.4V | 1. Attach a voltage source to the battery voltage sense pins<br>2. Sweep the voltage source from 5.0V to 9.0V<br>3. Verify that the BMS only attempts to charge the battery when the voltage is at or within the specified range of 8.4V to 5.4V | Verified (Section 3.4.2) |
| The BMS shall disconnect | 1. Attach a voltage source in place of the battery | Verified (Section 3.4.3) |

| | | |
|---|---|---|
| the battery if the load is shorted to ground | 2. Check that the BMS outputs the battery voltage<br>3. Short the output to ground<br>4. Verify that there is no current in the short | |
| The USB Serial Interface shall support a baud rate of at least 115200 | 1. Connect the I/O Board to a computer using a USB cable<br>2. Transmit known data to the I/O Board<br>3. Use an oscilloscope to determine the baud rate<br>4. Verify that the received data is the same as the transmitted data<br>5. Repeat the above procedure while transmitting data from the I/O Board | Verified (Section 3.2) |
| The Bluetooth SoC shall support Bluetooth Low Energy (BLE) 4.0 with a 5kbps transfer rate | 1. Pair the I/O Board with a BLE transceiver<br>2. Transmit a known amount of data to the Bluetooth SoC<br>3. Measure the transfer time to determine the transfer rate<br>4. Verify that the received data is the same as the transmitted data<br>5. Repeat the above procedure with the Bluetooth SoC transmitting | Verified (Section 3.1) |
| The Bluetooth SoC shall be capable of communicating with the EMG Board at a baud rate of at least 115200 | 1. Connect the I/O Board to the EMG Board<br>2. Transmit a known amount of data to the I/O Board<br>3. Measure the transmit time to determine the transfer rate<br>4. Verify that the received data is the same as the transmitted data<br>5. Repeat the above procedure while transmitting data to the EMG Board | Verified (Section 3.1) |
| The antenna shall have an input impedance of 50Ω +/- 5% at frequencies between 2400MHz and 2483.5MHz | 1. Attach a network analyzer to the matching network<br>2. Measure the reflection coefficient of the antenna at Bluetooth frequencies | Indirectly Verified (Section 3.1) |
| The matching network shall have an input impedance of 50Ω +/- 5% at between 2400MHz and 2483.5MHz on the antenna side | 1. Attach a network analyzer to the matching network<br>2. Measure the s-parameters of the network at Bluetooth frequencies<br>3. Calculate the input impedance from the reflection coefficient | Indirectly Verified (Section 3.1) |
| The matching network shall have an input impedance of 15+j85Ω +/- 5% at between 2400MHz and 2483.5MHz | 1. Attach a network analyzer to the matching network<br>2. Measure the s-parameters of the network at Bluetooth frequencies<br>3. Calculate the input impedance from the | Indirectly Verified (Section 3.1) |

| | | |
|---|---|---|
| on the Bluetooth SoC side | reflection coefficient | |

## Appendix B. Bill of Materials

| Description | Manufacturer Part Number | Qty. | Total (Qty. 5) | Total (Qty. 1k) |
|---|---|---|---|---|
| 10 µF, 25 V, X5R Ceramic Capacitor | TMK212BBJ106KG-T | 6 | $0.76 | $0.19 |
| 10 µF, 10 V, X5R Ceramic Capacitor | C0805C106K8PACTU | 5 | $0.47 | $0.10 |
| 1 µF, 25 V, X7R Ceramic Capacitor | CL10B105KA8NNNC | 2 | $0.12 | $0.03 |
| 47 nF, 25 V, X7R Ceramic Capacitor | TMK105B7473KV-F | 2 | $0.02 | $0.01 |
| 100 nF, 16 V, X7R Ceramic Capacitor | CL05B104KO5NNNC | 9 | $0.11 | $0.02 |
| 15 nF, 25 V, X7R Ceramic Capacitor | CC0402KRX7R8BB153 | 2 | $0.04 | $0.01 |
| 1 µF, 10 V, X7R Ceramic Capacitor | CL10B105KP8NNNC | 4 | $0.16 | $0.03 |
| 100 pF, 50 V, NP0 Ceramic Capacitor | GRM1555C1H101JA01D | 2 | $0.03 | $0.01 |
| 2.2 µF, 16 V, X5R Ceramic Capacitor | C0603C225K4PACTU | 1 | $0.12 | $0.02 |
| 33 pF, 50 V, NP0 Ceramic Capacitor | CL05C330JB5NNNC | 1 | $0.10 | $0.00 |
| 15 pF, 50 V, NP0 Ceramic Capacitor | CL05C150JB5NNNC | 1 | $0.10 | $0.00 |
| 1.8 nF, 50 V, NP0 Ceramic Capacitor | GRM1885C1H182JA01D | 1 | $0.11 | $0.02 |
| 680 pF, 50 V, NP0 Ceramic Capacitor | GRM1555C1H681JA01D | 1 | $0.04 | $0.01 |
| 3 pF, 50 V, NPO Ceramic Capacitor | CC0402CRNPO9BN3R0 | 2 | $0.03 | $0.01 |
| 1 nF, 25 V, X7R Ceramic Capacitor | CL05B102KA5NNNC | 1 | $0.10 | $0.00 |
| 2.2 pF, 50 V, NP0 Ceramic Capacitor | GRM1555C1H2R2BA01D | 1 | $0.03 | $0.01 |
| 4.7 µF, 10 V, X5R Ceramic Capacitor | CL10A475KP8NNNC | 3 | $0.13 | $0.05 |
| 1 pF, 50 V, NP0 Ceramic Capacitor | CL05C010BB5NNNC | 1 | $0.10 | $0.01 |
| 1.5 pF, 50 V, NP0 Ceramic Capacitor | GRM1555C1H1R5BA01D | 1 | $0.05 | $0.01 |
| 47 nF, 16 V, X7R Ceramic Capacitor | CL05B473KO5NNNC | 1 | $0.10 | $0.00 |
| 2.2 nF, 50 V, X7R Ceramic Capacitor | CL05B222KB5NNNC | 1 | $0.10 | $0.00 |
| 200 pF, 50 V, NP0 Ceramic Capacitor | CL05C201JB5NNNC | 2 | $0.03 | $0.02 |
| Red SMD LED | LTST-C191KRKT | 1 | $0.18 | $0.04 |
| Green SMD LED | LTST-C191KGKT | 1 | $0.18 | $0.04 |
| Orange SMD LED | LTST-C190KFKT | 1 | $0.16 | $0.04 |
| Blue SMD LED | LTST-C193TBKT-5A | 3 | $0.69 | $0.17 |
| 22 $V_{DC}$, 42.3$V_{ON}$, TVS Diode | SMBJ22A-TR | 1 | $0.16 | $0.08 |
| 3.3 $V_{DC}$, 13.7$V_{ON}$, TVS Diode | SMBJ6.0A-TR | 4 | $0.66 | $0.36 |
| 90Ω Ferrite Bead | ILHB0805ER900V | 1 | $0.08 | $0.03 |
| UMC Coaxial Connector | 734120110 | 1 | $0.58 | $0.37 |
| USB Type-C Mid-Mount Hybrid | 12401548E4#2A | 1 | $1.72 | $0.88 |
| 3.3 µH, 2.5 A, 28 mΩ Inductor | SRR6028-3R3Y | 1 | $0.74 | $0.46 |
| 3.3 nH, 2 A, 30 mΩ, Inductor | LQW15AN3N3B80D | 1 | $0.22 | $0.09 |
| 4.7 nH, 750 mA, 70 mΩ Inductor | LQW15AN4N7B00D | 1 | $0.16 | $0.07 |
| 10 nH, 500 mA, 170 mΩ Inductor | LQW15AN10NJ00D | 1 | $0.15 | $0.06 |
| 30 V, 25 A N-Type MOSFET | CSD17579Q5AT | 4 | $2.51 | $0.95 |
| 40 V, 6.4 A P-Type MOSFET | ZXMP4A16GTA | 1 | $0.84 | $0.35 |
| 1 Ω, 5%, 62.5 mW Resistor | RC0402JR-071RL | 2 | $0.02 | $0.00 |

| | | | | |
|---|---|---|---|---|
| 10 mΩ, 1%, 500 mW Resistor | CSR1206FK10L0 | 2 | $0.73 | $0.22 |
| 10 Ω, 1%, 100 mW Resistor | ERJ-2RKF10R0X | 5 | $0.10 | $0.02 |
| 100 kΩ, 5%, 62.5 mW Resistor | RC0402JR-07100KL | 2 | $0.02 | $0.00 |
| 300 kΩ, 5%, 62.5 mW Resistor | RC0402JR-07300KL | 1 | $0.10 | $0.00 |
| 1 kΩ, 5%, 62.5 mW Resistor | RC0402JR-071KL | 3 | $0.02 | $0.00 |
| 220 kΩ, 5%, 62.5 mW Resistor | RC0402JR-07220KL | 1 | $0.10 | $0.00 |
| 169 kΩ, 5%, 62.5 mW Resistor | ERJ-2RKF1693X | 1 | $0.00 | $0.00 |
| 40.2 kΩ, 5%, 62.5 mW Resistor | ERJ-2RKF4022X | 1 | $0.03 | $0.00 |
| 10 kΩ, 5%, 62.5 mW Resistor | RC0402JR-0710KL | 15 | $0.11 | $0.02 |
| 4.7 kΩ, 5%, 62.5 mW Resistor | RC0402JR-074K7L | 2 | $0.02 | $0.00 |
| 3.3 V, 150 mA LDO | TPS76333DBVT | 1 | $0.84 | $0.42 |
| 5.0 V, 150 mA LDO | TPS76350DBVT | 1 | $0.83 | $0.35 |
| 16.0000 MHz, 8 pF Crystal | CX3225GB16000D0HPQCC | 1 | $0.66 | $0.38 |
| BMS Controller IC | BQ25703ARSNT | 1 | $5.51 | $3.12 |
| Bluetooth Module IC | NRF51822-QFAA-T | 1 | $4.62 | $2.30 |
| USB Power Delivery IC | FUSB302MPX | 1 | $0.82 | $0.48 |
| DPDT Analog Switch | TS3A5223RSWR | 1 | $0.58 | $0.26 |
| USB to UART Converter IC | FT232RQ-REEL | 1 | $4.24 | $2.35 |
| $I^2C$ Temperature Sensor | TMP101NA/250 | 1 | $2.07 | $0.88 |
| **Totals** | | | **$33.48** | **$15.42** |